VIP Dynamic Materials

DOI: 10.1002/anie.200901670

Self-Healing Colloidal Crystals**

*Ashlee St. John Iyer and L. Andrew Lyon**

The self-assembly of colloidal building blocks is an important tool in the fabrication of photonic materials[1–3] and sensors,[4–6] where refractive index periodicity imparts advantageous optical properties. Well-defined colloidal materials have brought benefits to the field of condensed-matter physics,[7–9] as the large size and slow dynamics of colloidal particles provide an experimentally convenient model system for molecular interactions.[10] Colloidal particles used for these purposes range from hard-sphere materials such as poly(styrene),[5,8] poly(methyl methacrylate) (PMMA)[7,9] and silica,[2,11] as well as hybrid constructs[12–14] that combine multiple materials to tune the properties of the desired assembly. In this domain, solvent-swollen microgels have been of particular recent interest.[15–18] These particles interact through much softer interaction potentials than their hard-sphere counterparts, thereby dramatically increasing the richness of the resultant phase behavior. Herein, we present a remarkable example of the self-healing properties of microgel colloidal crystals in the presence of particle-size irregularity, which illustrates that such assemblies are intrinsically defect-tolerant because of their ability to dissipate defect energies over long distances through the lattice.

One of the characteristics of hard-sphere colloidal suspensions with respect to crystal formation is the strict requirement of monodispersed building blocks. Homogenous colloidal crystal nucleation is suppressed in colloidal suspensions with polydispersities greater than 10%,[19] and nucleated crystals rarely, if ever, exceed 5.7% polydispersity.[20,21] These values suggest that the lattice structure contains little or no tolerance for defects or dispersity in lattice constants. However, because of the soft and compressible nature of polymer microgels, it is reasonable to hypothesize that a crystal lattice assembled from microgels may display a certain degree of self-healing within the lattice structure. In this work, we have intentionally introduced large microgel "defects" into microgel assemblies, after which we probed the structure and dynamics in the defect region. We observed that the defect particles are seamlessly integrated into the bulk lattice with no observable perturbation of the lattice structure or dynamics. These observations suggest that self-healing is at play in microgel crystals, where microgel particles can adopt an optimal and uniformly narrow size distribution to accommodate the global energetic demands of the lattice.

Figure 1 shows the microgel building blocks under investigation. Figure 1a shows a brightfield transmission optical microscopy image of a crystalline assembly of poly(*N*-isopropylacrylamide-*co*-acrylic acid) microgels (pNIPAm–AAc, $R_h = (873 \pm 66)$ nm, 3.0 wt% dispersion). These large microparticles are packed to a volume fraction above their canonical freezing point (e.g., >50% fill fraction), thereby driving them into a crystalline assembly. Figure 1b shows a crystalline assembly composed of smaller poly(*N*-isopropylacrylamide) microgels (pNIPAm, $R_h = (357 \pm 20)$ nm, 5.5 wt% dispersion). However, the sample shown in Figure 1b is not composed exclusively of these smaller microgels, but has been doped with a small amount (ca. 0.1 wt%) of the larger pNIPAm–AAc microgels shown in Figure 1a. A dopant particle is present in the center of the image and has been encircled in white. In this image, the dopant is practically indistinguishable from the smaller particles surrounding it, as it has been compressed to accommodate the lattice constant dictated by the major component of the assembly. Experimentally, the only distinguishable feature of the dopant particles is a higher scattering cross-section, which arises from an increased refractive index contrast between the compressed defect particles and the surrounding water molecules. This increase results in brighter particles that produce a scattering halo, which is visible a few lattice planes above the particles and allows for their differentiation relative to the highly solvent swollen "bulk" particles.

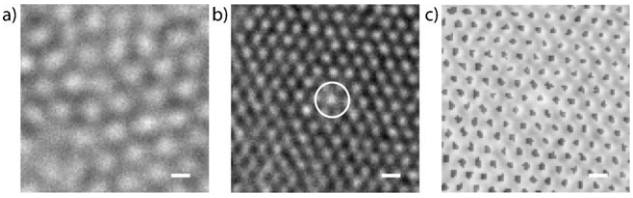

Figure 1. Optical micrographs of a) pNIPAm–AAc microgel particles (3 wt% polymer) dispersed in water, b) 3 mol% cross-linked pNIPAm particles (5.5 wt% polymer) dispersed with a single pNIPAm–AAc particle in the center (denoted by the white circle), and c) the assembly shown in (b) with the particle trajectories overlaid in grey. Scale bar = 1 μm.

The degree to which the assembly exerts control over the swelling behavior of the dopant particles is impressive considering that, in this particular example, the dopant particle occupies a volume that is approximately 15 times smaller than that observed in Figure 1a. In addition to the lack of structural disorder observed, Figure 1c shows the uniformity in diffusion dynamics observed in such assemblies.

[*] Dr. A. S. Iyer, Prof. L. A. Lyon
School of Chemistry and Biochemistry and Petit Institute for Bioengineering and Bioscience, Georgia Institute of Technology
Atlanta, GA 30332-0400 (USA)
Fax: (+1) 404-894-4090
E-mail: lyon@gatech.edu

[**] The authors thank Zhiyong Meng for providing the pNIPAm–AAc microgels and Profs. Victor Breedveld and Alberto Fernandez-Nieves for many valuable discussions. L.A.L. acknowledges support from the ACS-PRF.

The particle trajectories observed over approximately 15 seconds (20 frames s^{-1}) are shown as black lines overlaid upon the real-space image. The extents of the "defect" and bulk microgel trajectories are qualitatively indistinguishable from one another. Indeed, the trajectories illustrate that all particles have finite cages in which they diffuse. The particles are not strictly in close contact with their neighbors and are therefore not close-packed, that is, some solvent surrounds each particle to provide a significant amount of local mobility. The absence of close-packing, and the translational freedom thus afforded to the particles, is clearly demonstrated when compared with a truly close-packed assembly (Figure 2). Data

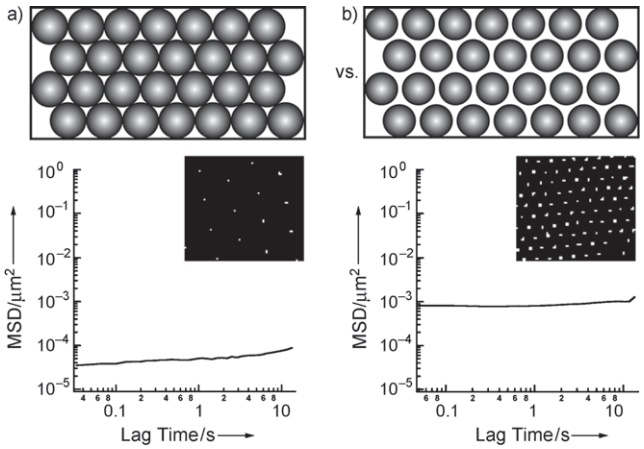

Figure 2. Illustration of crystalline assemblies of microgels at a) maximum packing fraction and b) just below maximum packing, with more translational freedom. Below the illustrations, MSD plots with associated particle trajectory maps (insets) are shown for a) 3.5 wt% sample of pNIPAm–AAc particles (pH 3.0, 10 mM ionic strength, $\phi_{eff} \approx 0.74$) and b) 3.8 wt% assembly of 1 mol% cross-linked pNIPAm particles ($\phi_{eff} \approx 0.86$).

obtained from a close-packed assembly of pNIPAm–AAc particles (3.5 wt% polymer, pH 3.0, 10 mM ionic strength, effective volume fraction $\phi_{eff} \approx 0.74$), which has previously been shown to adopt an arrangement in which the particles are truly in contact with one another, are shown in Figure 2a.[22] The close-packed structure is evident by the low diffusivity observed in the trajectories and mean squared displacement (MSD) data. Figure 2b shows a pNIPAm microgel assembly with trajectories and MSD values that indicate a significantly higher diffusivity than that found in the close-packed assembly. However, the pNIPAm crystal is actually a more densely packed assembly than that in Figure 2a, with respect to the degree of particle compression in the lattice (3.8 wt% polymer, $\phi_{eff} \approx 0.86$). As described below, an effective volume fraction greater than 0.74 indicates that the pNIPAm microgels have been forced to adopt a smaller volume than they attain in dilute solution.[23] In the close-packed pNIPAm–AAc case, the particles are highly restricted in their movement, as seen in the small displacement values and extremely tight trajectories. Conversely, the pNIPAm assembly is much more mobile, as the particles are not mechanically held in a singular lattice site by their neighbors, even though we would naively predict a rigid, tightly packed assembly based on simple volume fraction calculations (see below).

Considering the results shown in Figure 1, and the odd packing behavior illustrated in Figure 2, the origin of this self-healing phenomenon is still not immediately obvious. It is clear, however, that the lack of close particle contact argues against a purely mechanical deformation mechanism; that is, the dopant microgel is not simply "squeezed" by its nearest neighbors through particle–particle contacts. Instead, the seamless insertion of the defect into the lattice seems to be facilitated by noncontact forces, such as those that arise from osmotic effects in polymer solutions. The impact of external osmotic pressure on the swelling in polymeric gels has been well studied for both macroscopic gel and microgel particle systems.[24–28] A number of these investigations have focused on osmotic deswelling of microgels through the addition of linear polymers to the suspension.[29–31] Saunders and Vincent[30] have observed deswelling in pNIPAm microgel dispersions with poly(ethylene glycol) (PEG) as the polymeric additive, or osmolyte. Upon addition of PEG, the microgels underwent significant deswelling at PEG volume fractions as low as 0.1. Given these results, it may be the case that such effects also dictate the packing energetics in microgel assemblies. However, there are also a number of studies,[15,32–35] including our own,[23] that approach neutral microgel interactions solely from the perspective of the colloidal length scale. These studies assume or indirectly measure a short-ranged soft interaction potential between particles, and include no assumptions of long-range interactions such as osmotic deswelling. As discussed below, the data shown in Figures 1 and 2 suggest that the consideration of microgel assemblies in purely colloidal terms is a gross oversimplification; a combination of both colloidal and polymeric energetics conspires to dictate the structure and dynamics of the obtained phases.

To probe the generality of this phenomenon, we undertook studies of self-healing as a function of microgel concentration (packing density), which can be defined in terms of polymer composition (wt%), but are more applicable to discussions of phase behavior when converted to an effective volume fraction ϕ_{eff}. For microgels, the ϕ_{eff} value is obtained by fitting dilute solution viscosity data to Batchelor's equation,[36] thus obtaining a conversion factor that relates the polymer composition (wt%) to a ϕ_{eff} value.[33] This method of conversion is necessary because of the lack of a simple polymer-mass to particle-volume relationship in the highly solvent swollen microgels. The conversion factor is calculated from the dilute solution regime where there are virtually no particle–particle interactions. In more concentrated assemblies, a packing maximum is reached; as described above, this maximum is 74% for an face-centered-cubic crystal.[37] To accommodate higher microgel concentrations, the microgels must shrink, as the amount of solvent available is less than that required to reach the swelling limit of the microgels. Indeed, recent neutron scattering experiments clearly illustrate that long range interactions can contribute to deswelling in microgel suspensions and assemblies.[38] Decreases in the particle radius for a ϕ_{eff} value greater than 0.35 (well below

the maximum packing fraction of a crystal) and shifts in the peaks of the polymer density profiles were observed, which suggests the deswelling of the particles as a function of concentration. These data suggest that the present method for calculating values of ϕ_{eff} is not entirely accurate for 0.35–0.74, and can certainly be expected to diverge quickly from predicted values above 0.74. Accordingly, values of ϕ_{eff} above the packing maximum are no longer reasonable representations of the actual volume fraction of the assembly. They are, however, useful for providing a semi-quantitative picture of microgel "overpacking".

Micrographs and particle trajectory maps for crystals with a single central (circled) dopant pNIPAm–AAc microgel over a range of pNIPAm microgel concentrations are shown in Figure 3. The bulk pNIPAm microgels ($R_h = (357 \pm 20)$ nm) were synthesized to contain 3 mol% cross-linker and the crystals shown were prepared from various microgel concentrations. In this fashion, the assembly packing densities range from below the hard-sphere limit, to very overpacked assemblies with lattice constants smaller than the dilute solution microgel diameter. Figure 3 shows that as the overall microgel concentration is increased, there is a small but observable decrease in the apparent cage size available to each microgel, as would be expected with denser assemblies. Surprisingly, there is no observable difference in the cage sizes of the dopant particles versus the average bulk particles; the uniformity in structure and dynamics are preserved in the vicinity of the defect with no obvious perturbations. Similar experiments carried out using large pNIPAm particles ($R_h = (944 \pm 62)$ nm) as the dopant or defect resulted in qualitatively identical behavior (data not shown). Together, these observations strongly suggest that the dopant particle is experiencing compression because of the osmotic pressure of the highly concentrated microgel environment, and that short-range mechanical deformation is not operative in these assemblies.

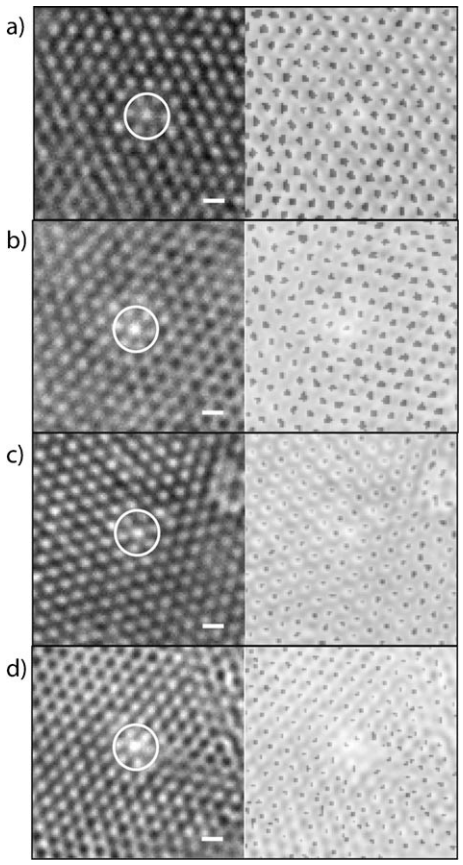

Figure 3. Optical micrographs (left) and trajectory overlays (right) of 3 mol% cross-linked pNIPAm microgel assemblies with a pNIPAm–AAc dopant in each image (circled). The pNIPAm assemblies have the following concentrations and volume fractions: a) ca. 5.5 wt% ($\phi_{eff} \approx 0.66$), b) ca. 5.8 wt% ($\phi_{eff} \approx 0.71$), c) ca. 6.4 wt% ($\phi_{eff} \approx 0.78$), and d) ca. 6.9 wt% ($\phi_{eff} \approx 0.84$). Scale bar = 1 μm.

Considering the forces involved in polymer gels, the total osmotic pressure inside a gel consists of mixing π_m, elastic π_e, and in some cases ionic π_i contributions.[39] In good solvents and within the weak screening limit, π_m and π_i contribute to gel swelling while π_e balances these contributions and controls the extent to which the gel is able to swell. At equilibrium, the sum of the contributions must be equal to the external osmotic pressure [Eq. (1)]:

$$\pi_{ext} = \pi_m + \pi_e \, \pi_i \tag{1}$$

The contribution from mixing is heavily dependent upon the Flory polymer–solvent interaction parameter χ, and is only varied substantially by changes in temperature or solvent [Eq. (2)]:[29,39]

$$\pi_m = -\frac{N_A k_B T}{v_s}\left[\phi + \ln(1-\phi) + \chi\phi^2\right] \tag{2}$$

where N_A is the Avogadro constant, k_B is the Boltzmann constant, T is temperature, and v_s is the molar volume of the solvent. The elastic contribution to swelling is [Eq. (3)]:

$$\pi_e = \frac{N_c k_B T}{v_0}\left[\frac{\phi}{2\phi_0} - \left(\frac{\phi}{\phi_0}\right)^{1/3}\right] \tag{3}$$

where N_c corresponds to the effective number of polymer chains in the gel, k_B is the Boltzmann constant, T is temperature, v_0 is the volume of the collapsed gel, ϕ_0 is the polymer volume fraction within the collapsed gel, and ϕ is the polymer volume fraction in the swollen gel. The elastic contribution is highly dependent on the polymer concentration, or segment density in the gel, which is directly related to the degree of gel swelling. When π_{ext} is increased, the sum of the internal pressure contributions must balance the external pressure by deswelling-induced increases in π_e.

In a concentrated solution of microgels, π_{ext} is largely controlled by the microgels themselves. If we approach their presence in solution as a purely polymeric contribution to π_{ext}, then that contribution should be equal to π_m over the entire system. If we assume $\chi = 0.4$, we obtain π_{ext} on the order of approximately 10^4 Pa. Considering that experimental values for the bulk elastic modulus of swollen microgels range from 10^2–10^4 Pa,[40,41] it is reasonable to consider osmotically induced deswelling as a considerable factor in the condensation of the dopant particles, and the associated

self-healing behavior. Furthermore, we might expect that more loosely cross-linked microgels should be more capable of interfacial interpenetration because of the presence of longer polymer chains at the microgel surface. Microgel–microgel interpenetration would reduce the impact of the solution osmotic pressure as compared to the more cross-linked particles used above, as chain interpenetration between microgels would increase the local segment density, and hence increase the internal osmotic pressure. Given this hypothesis, 1 mol% cross-linked pNIPAm microgels ($R_h = (395 \pm 11)$ nm) were synthesized and assembled with large dopant particles over a range of ϕ_{eff} values similar to those shown in Figure 3. Representative data from each concentration is shown in Figure 4. As with the data shown in Figure 3, the local structure and the particle mobility do not appear to be different in the vicinity of the dopant particle as compared with the surrounding particles, despite the significantly decreased cross-link density of the microgels that make up the bulk of the assembly. This observation either suggests that the 1 mol% assemblies do not strongly interpenetrate and still impose a large enough osmotic pressure to deswell the dopant particles, or that the polymeric concentration and concomitant osmotic deswelling is not the only relevant factor that contributes to the assembly self-healing. The latter possibility becomes the most plausible when we consider that the polymer concentration contribution does not fully address the differences we observe between assemblies. For instance, the samples in Figures 1a and 4a both consist of approximately 3 wt% polymer, but the pNIPAm–AAc particles are obviously experiencing two very different degrees of external pressure from the two different environments. In the homogeneous dispersion (Figure 1a), the microgels are free to adopt a swollen, space-filling arrangement, whereas when the pNIPAm–AAc microgels are used as dopants in pNIPAm lattices, both the osmolality of the solution and the colloidally imposed lattice constant appear to drive microgel deswelling.

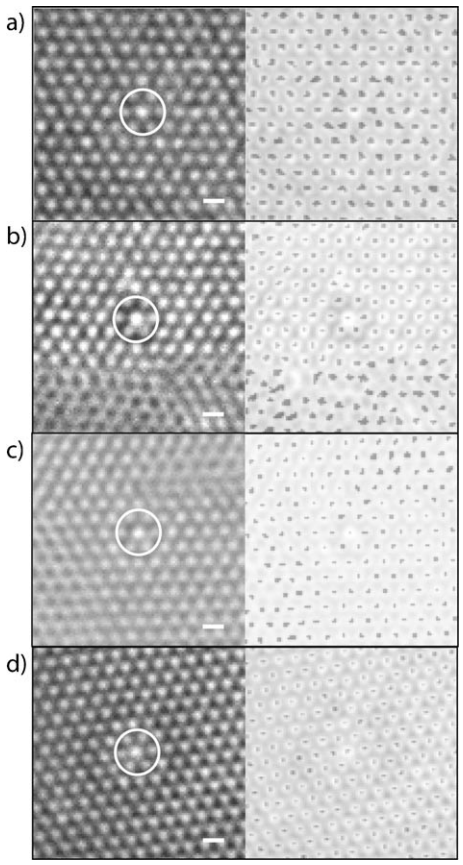

Figure 4. Optical micrographs (left) and trajectory overlays (right) of 1 mol% cross-linked pNIPAm microgel assemblies with a pNIPAm–AAc dopant in each image (circled). The pNIPAm assemblies have the following concentrations and volume fractions: a) ca. 2.9 wt% ($\phi_{eff} \approx 0.66$), b) ca. 3.2 wt% ($\phi_{eff} \approx 0.71$), c) ca. 3.4 wt% ($\phi_{eff} \approx 0.77$), and d) ca. 3.8 wt% ($\phi_{eff} \approx 0.86$). Scale bar = 1 μm.

Given these observations it is important to address the colloidal contributions to the osmotic pressure in the microgel assembly. In this case, $\pi_{ext} = n k_B T$, where n is the particle number density. Figure 1 shows $10 \times 10\ \mu m^2$ images; within the dimensions of these images the homogenous assembly of large microgels contains 40 particles, whereas the doped assembly of small microgels contains 164 particles. Assuming the samples were both assembled at the maximum packing fractions of 0.91 for two-dimensional hexagonally close-packed assemblies and 0.74 for three-dimensional face-centered-cubic crystals, a difference in microgel number densities of an order of magnitude exists between the two samples. For the sample in Figure 1a, $n = 0.28$ microgels μm^{-3}, whereas $n = 2.4$ microgels μm^{-3} for the sample in Figure 1b. Thus, the colloidal osmotic pressures alone are negligible in relation to observed microgel bulk moduli, but the significant difference between them suggests that they could also contribute to the difference in swelling behavior of the pNIPAm–AAc particles between the two samples. The exact manner in which the polymeric and colloidal characteristics of microgel assemblies work together to this end is unclear, but it is not unreasonable to assume, from the observations made in this study, that the colloidal number density functions as a form of scaling factor for the polymeric contribution to the external osmotic pressure of the system. Importantly, the observations detailed above make it clear that it is not possible to define microgel behavior by only polymer or colloidal characteristics. Microgel particles are both polymeric and colloidal in nature and the behaviors of assemblies created from these building blocks are subject to both physical characteristics. Whereas it is still unclear how polymer and colloid properties work together to dictate microgel assembly behavior, we have provided one example of how microgel complexity can translate to new and advantageous functionalities such as self-healing.

Experimental Section

Materials: The monomer *N*-isopropylacrylamide (NIPAm; Aldrich) was recrystallized from hexane (Fisher Scientific) prior to use. The cross-linker *N*,*N*′-methylenebis(acrylamide) (BIS; Aldrich), ammonium persulfate (APS; Aldrich), and acrylic acid (AAc; Fluka) were used as received. All water was purified to 18 MΩ with a Barnstead E-pure system.

Synthesis: Microgels were synthesized by precipitation polymerization[23] without the addition of surfactant in an aqueous solution (100 mL). The 3 mol% cross-linked pNIPAm microgel synthesis

contained NIPAm (1.537 g) and BIS cross-linker (0.065 g), and was initiated with APS (0.037 g). The 1 mol% cross-linked pNIPAm microgel synthesis contained NIPAm (1.569 g) and BIS cross-linker (0.028 g), and was initiated with APS (0.035 g). The 1 mol% cross-linked pNIPAm–AAc microgel synthesis contained NIPAm (1.8 g), BIS cross-linker (0.03 g), and AAc co-monomer (0.2 g), and was initiated with APS (0.05 g). Particles were purified by repeated centrifugation and resuspension.

Dynamic light scattering (DLS): The average hydrodynamic radius (R_h) and polydispersity of the particles at 20 °C were characterized by DLS (Wyatt Technology). Data are an average of 30 measurements with 30 s acquisition times. Samples were equilibrated for 10 min at 20 °C before measurements were taken. The average R_h of the particles was calculated from the measured diffusion coefficients by using the Stokes–Einstein equation. Diffusion coefficients were determined from the autocorrelation decay functions by using a regularization algorithm included in the manufacturer's software (Dynamics v6.9.2.9, Wyatt Technology).

Sample preparation: Homogeneous and doped samples containing varying concentrations of bulk microgels, and (for doped samples) 7 mL of a 1 wt% solution of dopant microgels were prepared and introduced into rectangular capillary tubes (VitroCom) that were then sealed to form a closed system as described previously.[42] The inner dimension of these capillaries is 100 μm along the imaging axis, and all microscopic observations were made approximately 50 μm into the sample, thus removing contributions that arise from the glass interface. Samples were allowed to equilibrate for at least 3 days after preparation before any measurements were taken.[23]

Microscopy and particle tracking: Particle assemblies were imaged on an Olympus IX71 microscope with a 100× oil immersion objective (1.3 N.A.) in bright field (DIC mode). Images were recorded with Andor Luca EMCCD (Image resolution: 100 μm pixel^{-1}). Samples were maintained at room temperature, approximately 20 °C, during all experiments. Images were recorded at 20 frames s^{-1} for 15 s. The obtained image time series were then analyzed on IDL image analysis software (Research Systems, Inc.) with a modified form of particle-tracking routines originally developed by Crocker and Grier.[43] Image analysis established particle position maps from which particle trajectories and MSDs were calculated.

Received: March 27, 2009
Published online: May 19, 2009

Keywords: colloids · gels · polymers · self-assembly · self-healing

[1] G. A. Ozin, S. M. Yang, *Adv. Funct. Mater.* **2001**, *11*, 95.
[2] A. van Blaaderen, R. Ruel, P. Wiltzius, *Nature* **1997**, *385*, 321.
[3] Y. A. Vlasov, X. Z. Bo, J. C. Sturm, D. J. Norris, *Nature* **2001**, *414*, 289.
[4] J. H. Holtz, S. A. Asher, *Nature* **1997**, *389*, 829.
[5] R. A. Potyrailo, Z. B. Ding, M. D. Butts, S. E. Genovese, T. Deng, *IEEE Sens. J.* **2008**, *8*, 815.
[6] E. T. Tian, J. X. Wang, Y. M. Zheng, Y. L. Song, L. Jiang, D. B. Zhu, *J. Mater. Chem.* **2008**, *18*, 1116.
[7] U. Gasser, E. R. Weeks, A. Schofield, P. N. Pusey, D. A. Weitz, *Science* **2001**, *292*, 258.
[8] D. G. Grier, C. A. Murray, *J. Chem. Phys.* **1994**, *100*, 9088.
[9] P. N. Pusey, W. Van Megen, *Nature* **1986**, *320*, 340.
[10] Liquids, Freezing, and Glass Transition, Pt. 2, Session LI, Les Houches Summer School Proceedings 1989 (Eds.: J. P. Hansen, D. Levesque, J. Zinn-Justin), **1991**.
[11] H. J. Kim, S. Kim, H. Jeon, J. Ma, S. H. Choi, S. Lee, C. Ko, W. Park, *Sens. Actuators B* **2007**, *124*, 147.
[12] I. Gorelikov, L. M. Field, E. Kumacheva, *J. Am. Chem. Soc.* **2004**, *126*, 15938.
[13] J. G. McGrath, R. D. Bock, J. M. Cathcart, L. A. Lyon, *Chem. Mater.* **2007**, *19*, 1584.
[14] D. Suzuki, J. G. McGrath, H. Kawaguchi, L. A. Lyon, *J. Phys. Chem. C* **2007**, *111*, 5667.
[15] A. M. Alsayed, M. F. Islam, J. Zhang, P. J. Collings, A. G. Yodh, *Science* **2005**, *309*, 1207.
[16] T. Cai, G. N. Wang, S. Thompson, M. Marquez, Z. B. Hu, *Macromolecules* **2008**, *41*, 9508.
[17] T. Hellweg, C. D. Dewhurst, E. Bruckner, K. Kratz, W. Eimer, *Colloid Polym. Sci.* **2000**, *278*, 972.
[18] L. A. Lyon, J. D. Debord, S. B. Debord, C. D. Jones, J. G. McGrath, M. J. Serpe, *J. Phys. Chem. B* **2004**, *108*, 19099.
[19] S. Auer, D. Frenkel, *Nature* **2001**, *413*, 711.
[20] P. G. Bolhuis, D. A. Kofke, *Phys. Rev. E* **1996**, *54*, 634.
[21] D. A. Kofke, P. G. Bolhuis, *Phys. Rev. E* **1999**, *59*, 618.
[22] Z. Meng, J. K. Cho, V. Breedveld, L. A. Lyon, *J. Phys. Chem. B* **2009**, *113*, 4590.
[23] A. N. St. John, V. Breedveld, L. A. Lyon, *J. Phys. Chem. B* **2007**, *111*, 7796.
[24] B. H. Tan, K. C. Tam, Y. C. Lam, C. B. Tan, *Langmuir* **2005**, *21*, 4283.
[25] B. R. Saunders, H. M. Crowther, G. E. Morris, S. J. Mears, T. Cosgrove, B. Vincent, *Sens. Actuators A* **1999**, *149*, 57.
[26] H. Inomata, K. Nagahama, S. Saito, *Macromolecules* **1994**, *27*, 6459.
[27] F. Horkay, I. Tasaki, P. J. Basser, *Biomacromolecules* **2000**, *1*, 84.
[28] J. Bastide, S. Candau, L. Leibler, *Macromolecules* **1981**, *14*, 719.
[29] A. Fernandez-Nieves, A. Fernandez-Barbero, B. Vincent, F. J. de Las Nieves, *J. Chem. Phys.* **2003**, *119*, 10383.
[30] B. R. Saunders, B. Vincent, *J. Chem. Soc. Faraday Trans.* **1996**, *92*, 3385.
[31] B. R. Saunders, B. Vincent, *Colloid Polym. Sci.* **1997**, *275*, 9.
[32] J. Wu, B. Zhou, Z. Hu, *Phys. Rev. Lett.* **2003**, *90*, 048304.
[33] H. Senff, W. Richtering, *J. Chem. Phys.* **1999**, *111*, 1705.
[34] H. Senff, W. Richtering, *Colloid Polym. Sci.* **2000**, *278*, 830.
[35] S. E. Paulin, B. J. Ackerson, M. S. Wolfe, *J. Colloid Interface Sci.* **1996**, *178*, 251.
[36] G. K. Batchelor, *J. Fluid Mech.* **1976**, *74*, *Pt.1*, 1.
[37] G. D. Scott, *Nature* **1960**, *188*, 908.
[38] M. Stieger, J. S. Pedersen, P. Lindner, W. Richtering, *Langmuir* **2004**, *20*, 7283.
[39] P. J. Flory, *Principles of Polymer Chemistry*, Cornell University Press, Ithaca, **1953**.
[40] O. Tagit, N. Tomczak, G. J. Vancso, *Small* **2008**, *4*, 119.
[41] J. Wiedemair, M. J. Serpe, J. Kim, J. F. Masson, L. A. Lyon, B. Mizaikoff, C. Kranz, *Langmuir* **2007**, *23*, 130.
[42] S. B. Debord, L. A. Lyon, *J. Phys. Chem. B* **2003**, *107*, 2927.
[43] J. C. Crocker, D. G. Grier, *J. Colloid Interface Sci.* **1996**, *179*, 298.

